Journal of Physics: Conference Series

PAPER • OPEN ACCESS

# An Intelligent Automatic Fault Detection Technique Incorporating Image Processing and Fuzzy Logic

To cite this article: Kulsoom Iftikhar *et al* 2019 *J. Phys.: Conf. Ser.* **1244** 012035

# An Intelligent Automatic Fault Detection Technique Incorporating Image Processing and Fuzzy Logic

**Kulsoom Iftikhar, Shahzad Anwar*, Muhammad Tahir Khan**
Department of Mechatronics Engineering, University of Engineering and Technology Peshawar, Pakistan

**Yasser Abd. Djawad**
Department of Electronics Engineering, Universitas Negeri Makassar, South Sulawesi, Indonesia

*Corresponding author: Shahzad.anwar@uetpeshawar.edu.pk

**Abstract.** Fault detection is considered an important and challenging task to be incorporated in many industrial applications. It has gained interest in recent years, and many techniques have been proposed for developing an effective fault detection approach due to its significant importance in everyday life. This study presents an automated intelligent fault detection technique incorporating image processing and fuzzy logic. Image processing is the first step where features such as entropy estimation, color-based segmentation and depth estimation from gradients are obtained. The extracted features (number of {blobs, minima, maxima}, and estimated entropy) act as input to the fuzzy logic. The subsequent step incorporates fuzzy logic; the four inputs are fed to fuzzy which extract the fault and acts as knowledge rule-based tool and final step, i.e. the output generation, classifies it accordingly into four categories of faults (rust, bumps, hole, wrinkles/roller marks). The proposed method is compared with Linear Vector Quantization, and Multivariate Discriminant Function approaches. The method is tested on a database of 150 images. The proposed method demonstrated its significance and effectiveness with performance accuracy of 99%, 98%, 96.8% and 97.6% for rust, bumps, holes and wrinkles/roller marks respectively.

**Keywords**: fault detection, image processing, fuzzy logic

## 1. Introduction

Machines, processes and equipment act as a fundamental platform in industrial manufacturing to produce economically high-quality products in required volumes [1]. As the manufacturing processes and machines are becoming complex, effective and efficient schemes are required equipment that can inspect faults to avoid enormous failures and breakdowns [2]. Some faults are visible and can easily be detected with the naked human eye. However, faults can arise that are not visible to the human eye, and special methods are required to detect these faults. Therefore, in time online detection and extraction of fault are very necessary to avoid further complications [3].

The defected parts can be recycled to make fault free parts, and the wastage of material can be reduced. The first is a mature linear method but unable due to shortcomings and localization to detect the characteristics of the manufacturer [4]. Second is artificial intelligence which incorporates artificial neural network [5][6] fuzzy logic [7], genetic algorithms [8], expert systems [9], reasoning based systems [10], etc. However, some of these methods require previous knowledge and training data [4]. Fuzzy logic imitates the human brain's logic and expresses it in the form of rules for decision making by the computer in the shape of an algorithm. It has been utilized in many areas for fault detection like robotics, machine vision, energy, mechanics, industries, etc [11]. Image processing and threshold-based decision techniques are also used for fault detection [3]. There are six categories of threshold techniques [12], i.e. histogram shape based, clustering shape based, entropy-based, image attribute based, spatial based and local characteristics based approaches.

Numerous approaches and techniques have been proposed in the literature for fault detection in various fields. A fuzzy logic based diagnosis system [11] was proposed for the detection of faults in power circuit breakers. Information about the monitored equipment was acquired by fuzzy logic, and an alarm would generate if the fault was present in the equipment. Defects in the textiles were detected by proposing a scheme in [13] by incorporating gray level co-occurrence matrix (GLCM), wavelet transforms and adaptive neuro-fuzzy inference system. In [14] a hybrid intelligent system incorporating fuzzy c-means clustering and artificial immune system approaches was proposed. Dimce et al. [15] proposed an approach for the estimation of the depth map of an image by integration of the estimated depth gradients utilizing maximum a posteriori probability (MAP). The approach observed the relationship between low-level image features and depth gradients utilizing supervised machine learning. Sinha et al. [16] proposed a neuro-fuzzy scheme to detect faults in pipes. The scheme incorporated fuzzification of input features of images and then fed to the neural network module for classification purpose. Alam et al. [17] designed a fault detection technique based on image processing to detect faults in industrial pipes. Islam et al. [18] developed a method which deals with the image acquisition of the inner surface of cylindrical pipes. Ganjdanesh et al. [19] proposed a fault detection and diagnosis scheme for the comparison of faulty and non-faulty data of a plant. The comparison was made between fuzzy reference models and fuzzy partial trained plant data. D'Angelo et al. [20] formulated a three-step approach incorporating Kohonen neural network classification algorithm, fuzzy clustering and Metropolis-Hastings algorithm for the detection of an induction machine stator-winding fault. Zhai et al. [21] proposed a fault detection scheme for long-term prediction of faults in gas turbines utilizing self-organizing fuzzy neural networks (SOFNN).

## 2. Proposed Methodology

In this study, a fault detection scheme has been proposed incorporating image processing and fuzzy logic. The proposed methodology incorporates three steps; image processing, fuzzy logic and output generation. The proposed scheme is depicted in the following Figure 1.

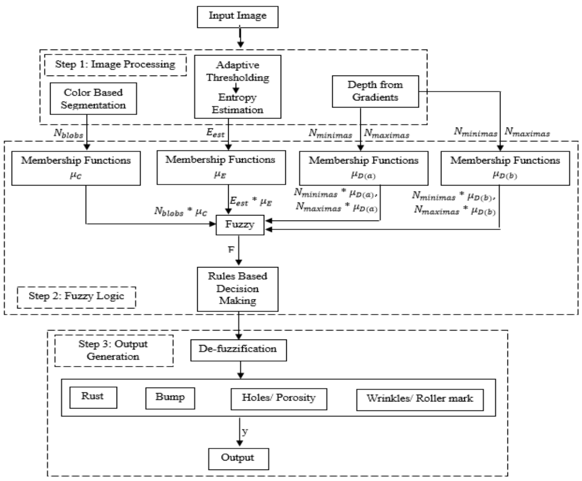


**Figure 1.** A detailed flow chart representing the steps involved in the methodology

IOP Conf. Series: Journal of Physics: Conf. Series **1244** (2019) 012035 doi:10.1088/1742-6596/1244/1/012035

### *2.1. Image processing*
An image was given as input to the image processing step incorporating three techniques, i.e. color based segmentation, depth estimation from gradients using Frankot Chellappa algorithm [22] and entropy estimation. These approaches were used to extract features from the input image and fed them to step 2, i.e. fuzzy logic.

### *2.2. Color based segmentation*
In this approach, first, the image was converted from RGB to Hue, Saturation, and Value (HSV) format. The H, S, V images (hImage, sImage, vImage) were extracted, and thresholds were assigned to them separately as shown in Table 1.

**Table 1.** Assigned upper and lower threshold values to the (HSV) images separately

| HSV image | Upper and lower limits | Threshold (T) value assigned |
|---|---|---|
| Hue | Low (HTL) | 0.003 |
| | High (HTHi) | 0.091 |
| Saturation | Low (STL) | 0.3 |
| | High (STHi) | 1 |
| Value | Low (VTL) | 0.1 |
| | High (VTHi) | 0.5 |

Based on the threshold values assigned to HSV images separately as shown in Table 1, (H, S, V) masks were generated and integration of the three masks was performed based on certain rules to obtain the region where all the three masks were true, shown in Table 2. Color based segmentation results were derived for a rusty image as shown in Figure 2.

**Table 2.** Rules for the Generation and Integration of (H, S, V) Masks

| Mask type | Rules for generation of masks |
|---|---|
| Hue | (hImage ≥ HTL) & (hImage ≤ HTHi) |
| Saturation | (sImage ≥ STL) & (sImage ≤ STHi) |
| Value | (vImage ≥ VTL) & (hImage ≤ VTHi) |

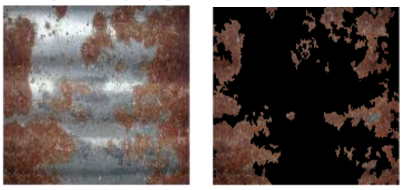

(a) (b)

**Figure 2.** Comparison between the original input image and the extracted rusty regions of the image (a) rusty image, (b) the extracted rusty regions of the image rusty

### *2.3. Depth estimation from gradients*
Depth estimation from gradients Frankot Chellappa algorithm was adopted in this study to extract two vital features from the image. To calculate the number of blobs, peaks were calculated in the cut off-depth image as peaks represent blobs in the current scenario. Figure 3 (a) represents the original image with estimated depths from gradients, and Figure 3 (b) depicts the processed image after the implementation of cutoffs in which the unwanted peaks were removed from the image.

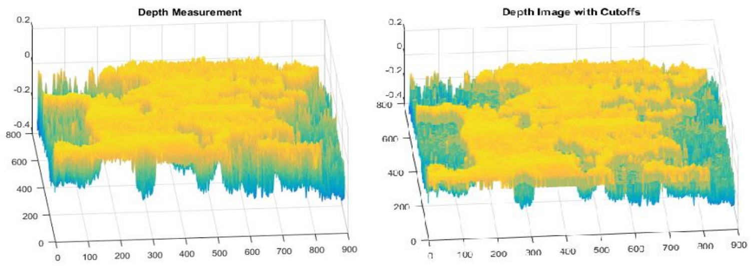


(a) (b)

**Figure 3.** (a) Original depth graph estimated from the gradients; (b) Depth image obtained after the implementation of cutoffs

### *2.4. Entropy estimation of the image*

At the end of the first step of the methodology, i.e. the image processing step, four features were extracted (number of {blobs, minima, maxima}, estimated entropy) from the input image. These features act as input to the fuzzy logic in the second step of methodology, explained under the fuzzy logic section.

### *2.5. Fuzzy logic*

In this step, a Fuzzy Inference System (FIS) was designed to simulate the output. The FIS was designed to contain eight variables both input features (number of {blobs, maxima, minima}, estimated entropy) and outputs (rust, bumps, holes, wrinkles/roller marks). Membership functions were generated for each variable as shown in Table 3. These membership functions were integrated with each feature's output and given to fuzzy as input. Seven rules were defined for the rule-based decision making which is depicted in Table 4.

**Table 3.** FIS variables and defined membership functions

| | Fis variable | Defined membership function |
|---|---|---|
| INPUTS | Number of Blobs | None, Few |
| | Number of Maxima | None, Few, Many |
| | Number of Minima | None, Few, Many |
| | Estimated Entropy | None, Low, Medium, High |
| OUTPUTS | Rust | No Rust, Rust |
| | Bumps | No Bumps, Bumps |
| | Holes | No hole, Few holes |
| | Wrinkles/roller marks | No Marks, Marks |

**Table 4.** Rules defined for rule-based decision making for fuzzy

| S. No | Number of blobs (none, few) | Number of maxima (none, few, many) | Number of minima (none, few, many) | Entropy (none, low, medium, high) | Result |
|---|---|---|---|---|---|
| 1 | Few | None | None | None | Rust |
| 2 | None | Few | None | None | Bump |
| 3 | None | Many | None | None | Bump |
| 4 | None | None | Few | None | Hole |
| 5 | None | None | Many | None | Porosity |
| 6 | None | Many | Many | High | Wrinkling/ roller mark |
| 7 | None | None | None | None | No Defect |

The proposed methodology is designed in such a way that it can differentiate between holes and porosity. The range specified at the output for the hole was (≥ 0.45) and (< 0.45) was defined to be porosity. The fuzzy logic model with input and output variables along with their defined membership functions is depicted in the following Figure 4 and Table 5 respectively.

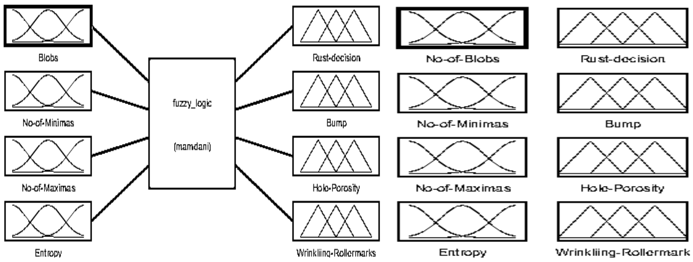


(a) (b)

**Figure 4.** (a) Shows the Fuzzy Logic Model designed with Mamdani type Fuzzy Inference (FIS), (b) shows the eight FIS variables defined in the scheme, input variables are shown in the left column and output variables in the right column

**Table 5.** The defined membership functions of the Fuzzy Inference System of input and output variables

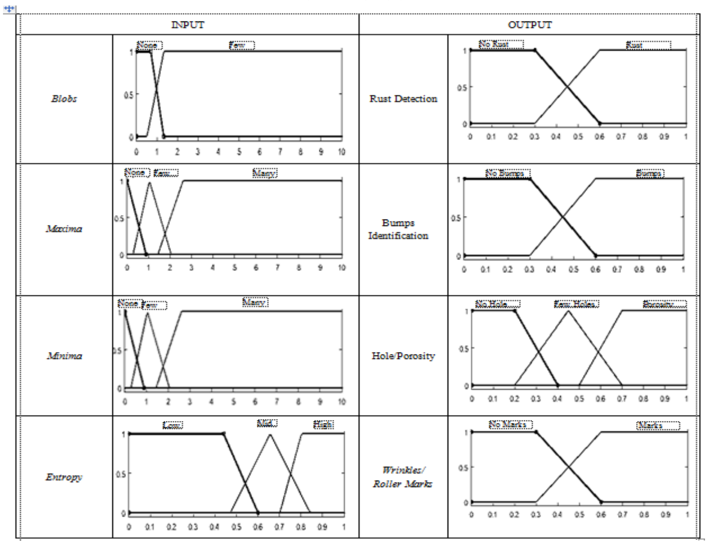


## 3. Result and Simulations

Random defected images freely available [23][24][25] were included later; the more challenging image was chosen to be tested for the designed scheme. The results obtained from the proposed scheme are summarized under four categories, i.e. rust, bumps, wrinkles/roller marks, and holes detection.

### *3.1. Rust detection*

For rust detection, first, a simple image was taken followed by a more challenging image and given as input to the methodology. Figure 5 shows the original image with rust patches on it and the output image generated after the implementation of the proposed methodology technique. The rust patches have been efficiently separated as faulty segments in the image.

IOP Conf. Series: Journal of Physics: Conf. Series **1244** (2019) 012035 doi:10.1088/1742-6596/1244/1/012035

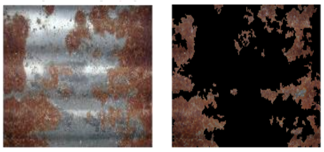

**Figure 5.** Rust detection

**Table 6.** Data obtained from the depth measurement of gradients, rust detection, entropy estimation and the output decision generated after the application of image processing and fuzzy logic

| | | | | | | |
|---|---|---|---|---|---|---|
| Depth from Gradients | No. of Maxima | No. of Minima | MSV | Max Value | Min Value | |
| | 355 | 419 | $2.435\times10^{-3}$ | $1.437\times10^{-1}$ | $3.014\times10^{-1}$ | |
| Entropy Estimation | Original image | | | Processed image | | |
| | 7.293184 | | | $7.056794\times10^{-1}$ | | |
| Rust Detection | | Blob Number | Area in Pixels | Mean | | |
| | | | | H | S | V |
| | SUM | 26 | 181358 | 1.520 | 11 | 11.47 |
| Output Decision | Rust | Bumps | Holes | | Wrinkles/ Roller marks | |
| | 0.7208 | 0.2307 | 0.1530 | | 0.2307 | |

(MSV= mean surface value, Max= maximum, Min= minimum H= hue, S= saturation, V= value)

*3.2. Bump identification*

The second category of faults was bumps identification as shown in Figure 6 (a) and the simulated results are illustrated in Figure 6 (b). The obtained result further validated the accuracy of the proposed method as shown in Table 7 (Rust detection). The maximum output obtained from the algorithm was for the bump as shown in Table 7. Hence, the fault was detected as a bump in the input image.

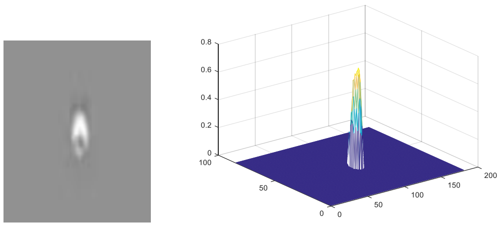

(a) (b)

**Figure 6.** (a) Shows the original image showing a single bump; (b) Shows the depth image obtained.

**Table 7.** Data obtained from the depth measurement of gradients of bump image, entropy estimation, rust detection algorithm and the final output decision generated after the application of image processing and fuzzy logic

| | | | | | | |
|---|---|---|---|---|---|---|
| Depth from Gradients | No. of Maxima | No. of Minima | MSV | Max Value | Min Value | |
| | 2 | 0 | $1.018\times10^{-2}$ | $7.151\times10^{-1}$ | $-1.167\times10^{-1}$ | |
| Entropy Estimation | Original image | | | Processed image | | |
| | $7.919927\times10^{-1}$ | | | $9.468119\times10^{-2}$ | | |
| Rust Detection | | Blob Number | Area in Pixels | Mean | | |
| | | | | H | S | V |
| | SUM | 0 | 0 | 0 | 0 | 0 |
| Output Decision | Rust | Bumps | Holes | | *Wrinkles/ Roller marks* | |
| | 0.2631 | 0.6872 | 0.1745 | | 0.2631 | |

### *3.3. Wrinkles detection*

The original image and the obtained adaptive threshold versions of the image are shown in Figure 7 (a) and the pattern obtained from the image containing wrinkles utilizing the depth from gradients is shown in Figure 7 (b).The results obtained by utilizing the entropy estimation and depth from gradients were summarized in Table 8. The maximum output obtained was classified as wrinkles in the input image.

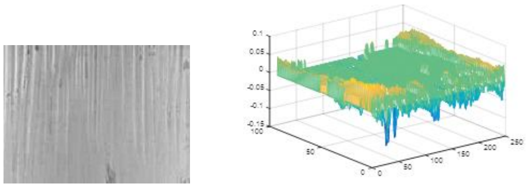

(a) (b)

**Figure 7.** (a) Shows the converted grey image as input; (b) Shows the depth image obtained after the implementation of cut-offs

**Table 8.** Data obtained from the depth measurement of gradients of wrinkled metal sheet image, entropy estimation, rust detection and the output generated after the application of image processing and fuzzy logic

| | | | | | | |
|---|---|---|---|---|---|---|
| Depth from Gradients | No. of Maxima | No. of Minima | MSV | Max Value | Min Value | |
| | 74 | 68 | $-1.474\times10^{-1}$ | $4.353\times10^{-1}$ | $-3.901\times10^{-1}$ | |
| Entropy Estimation | Original image | | | Processed image | | |
| | 5.734868 | | | $8.119075\times10^{-1}$ | | |
| Rust Detection | | Blob Number | Area in Pixels | Mean | | |
| | | | | H | S | V |
| | SUM | 0 | 0 | 0 | 0 | 0 |
| Output Decision | Rust | Bumps | Holes | | Wrinkles/ Roller marks | |
| | 0.2307 | 0.2307 | 0.1530 | | 0.7208 | |

### *3.4. Roller marks detection*

The same procedure was repeated for the roller marks detection as earlier explained with the original input image shown in Figure 8 (a), results obtained illustrated in Figure 8 (b) respectively and summarized as shown in Table 9. As evident from Table 9, the fault detected using the proposed methodology was roller marks as the output obtained under the fourth category was maximum.

**Table 9.** Data obtained from the depth measurement of gradients of roller marks image, entropy estimation, rust detection and the output generated after the application of image processing and fuzzy logic

| | | | | | | |
|---|---|---|---|---|---|---|
| Depth from Gradients | No. of Maxima | No. of Minima | MSV | Max Value | Min Value | |
| | 466 | 305 | $-2.884\times10^{-1}$ | 4.45×10 -1 | $-4.461\times10^{-1}$ | |
| Entropy Estimation | Original image | | | Processed image | | |
| | 6.655783 | | | $9.334746\times10^{-1}$ | | |
| Rust Detection | | Blob Number | Area in Pixels | Mean | | |
| | | | | H | S | V |
| | SUM | 0 | 0 | 0 | 0 | 0 |
| Output Decision | Rust | Bumps | Holes | | Wrinkles/ Roller marks | |
| | 0.2307 | 0.2307 | 0.1530 | | 0.7208 | |

IOP Conf. Series: Journal of Physics: Conf. Series **1244** (2019) 012035 doi:10.1088/1742-6596/1244/1/012035

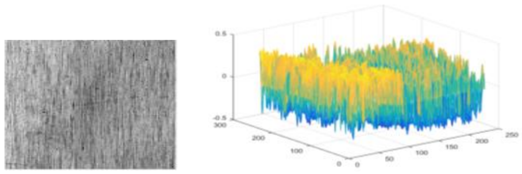

(a) (b)

**Figure 8.** (a) Shows the input image with roller marks; (b) Shows the depth image obtained after applying cutoffs

*3.5. Holes Detection*

The input image with a hole was fed to rust detection algorithm which showed zero readings at the output as illustrated in Table 10 (rust detection). The values obtained after the implementation of entropy estimation and depth gradients have been summarized in Table 10. The fault as illustrated in Table 10 with an output value of 0.45 was detected as a hole.

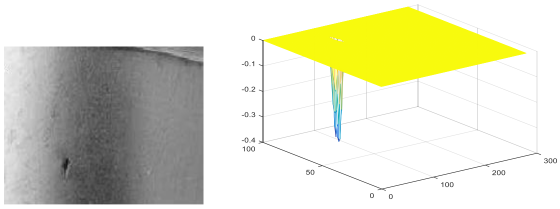

(a) (b)

**Figure 9.** (a) Shows the original input image with a hole; (b) Shows the extracted hole in the depth image with cut offs

**Table 10.** Data obtained from the depth measurement of gradients of hole image, entropy estimation, rust detection and the output generated after the application of image processing and fuzzy logic

| | | | | | | |
|---|---|---|---|---|---|---|
| Depth from Gradients | No. of Maxima | No. of Minima | MSV | Max Value | Min Value | |
| | 0 | 1 | $4.22\times10^{-3}$ | $5.78\times10^{-2}$ | $-3.983\times10^{-1}$ | |
| Entropy Estimation | Original image | | | Processed image | | |
| | 7.080996 | | | $4.396403\times10^{-1}$ | | |
| Rust Detection | | Blob Number | Area in Pixels | Mean | | |
| | | | | H | S | V |
| | SUM | 0 | 0 | 0 | 0 | 0 |
| Output Decision | Rust | Bumps | Holes | | Wrinkles/ Roller marks | |
| | 0.2337 | 0.2337 | 0.4500 | | 0.2337 | |

To check the performance accuracy and effectiveness of the proposed scheme, a comparison is drawn between approaches illustrated in Table 11, i.e. Learning Vector Quantization (LVQ) [26], Multivariate Discriminant Function (MDF) [27] and the developed scheme. It is evident from Table 11 that the proposed method incorporating image processing and fuzzy logic is efficient and detects faults with higher percentage accuracy as compared to the illustrated classification methods (LVQ [26] and MDF [27]).

**Table 11.** Comparison between the proposed method, learning vector quantization and multivariate discriminant function methods

| Types of Defects | Percentage Accuracy (%) | | |
|---|---|---|---|
| | LVQ [26] | MDF [27] | Proposed Method |
| Rust | 68 | N/A | 99 |
| Bumps | 88 | N/A | 98 |
| Hole | 88 | N/A | 96.8 |
| Roller marks | 71 | N/A | 97.6 |
| Wrinkles | N/A | 91 | 97.6 |

(LVQ= Learning Vector Quantization, MDF= Multivariate Discriminant Function)

## 4. Conclusion

In this study, a methodology has been proposed for the detection and classification of faults. The proposed scheme has been designed to incorporate two important approaches, i.e. image processing and fuzzy logic. The image processing step extracted essential features (number of blobs, maxima, minima, estimated entropy) from the input image by the utilization of three approaches. The features were fed as input to fuzzy which comprised of a fuzzy inference system (FIS). The utilization of the FIS and rule-based decision results in the detection and classification of fault into the four categories such as rust, bump identification, hole, wrinkles/roller marks detection). The proposed scheme has been implemented on a database of fifty images. The results generated were very accurate and showed the efficiency and accuracy of the proposed scheme.

## Reference

[1] S. Mellor, L. Hao, and D. Zhang, "Additive manufacturing: A framework for implementation," *Int. J. Prod. Econ.*, vol. 149, pp. 194–201, 2014.
[2] N. Bayar, S. Darmoul, S. Hajri-Gabouj, and H. Pierreval, "Fault detection, diagnosis and recovery using Artificial Immune Systems: A review," *Eng. Appl. Artif. Intell.*, vol. 46, pp. 43–57, 2015.
[3] G. K. Choudhary and S. Dey, "Crack detection in concrete surfaces using image processing, fuzzy logic, and neural networks," in *Advanced Computational Intelligence (ICACI), 2012 IEEE Fifth International Conference on*, 2012, pp. 404–411.
[4] Y. Ling, X. Xu, L. Shen, and J. Liu, "Multi sensor data fusion method based on fuzzy neural network," in *Industrial Informatics, 2008. INDIN 2008. 6th IEEE International Conference on*, 2008, pp. 153–158.
[5] R. Perla, S. Mukhopadhyay, and A. N. Samanta, "Sensor fault detection and isolation using artificial neural networks," in *TENCON 2004. 2004 IEEE Region 10 Conference*, 2004, vol. 500, pp. 676–679.
[6] K. Iftikhar, S. Anwar, I. U. Haq, M. T. Khan, and S. R. Akbar, "An Optimal Neural Network Based Classification Technique for Breast Cancer Detection," *J. Eng. Appl. Sci.*, vol. 35, no. 1, pp. 51–58, 2016.
[7] S. O. Ibrahim and E. A. Elzahab, "Implementation of fuzzy modeling system for faults detection and diagnosis in three phase induction motor drive system," *J. Electr. Syst. Inf. Technol.*, vol. 2, no. 1, pp. 27–46, 2015.
[8] X.-Z. Gao, S. J. Ovaska, and Y. Dote, "Motor fault detection using Elman neural network with genetic algorithm-aided training," in *Systems, Man, and Cybernetics, 2000 IEEE International Conference on*, 2000, vol. 4, pp. 2386–2392.
[9] A. Khosravi, H. A. Talebi, and M. Karrari, "Fault detection and isolation for unknown nonlinear systems using expert methods," in *Control Applications, 2005. CCA 2005. Proceedings of 2005 IEEE Conference on*, 2005, pp. 1485–1490.
[10] A. Bregon *et al.*, "Focusing fault localization in model-based diagnosis with case-based reasoning," in *Control Conference (ECC), 2007 European*, 2007, pp. 2312–2318.

[11] M. Andruşcă, M. Adam, A. Baraboi, A. Dragomir, and A. Munteanu, "Using fuzzy logic for diagnosis of technical condition of power circuit breakers," in *Electrical and Power Engineering (EPE), 2014 International Conference and Exposition on*, 2014, pp. 268–273.
[12] M. Thakkar and H. Shah, "Automatic thresholding in edge detection using fuzzy approach," in *Computational Intelligence and Computing Research (ICCIC), 2010 IEEE International Conference on*, 2010, pp. 1–4.
[13] B. Venkatesan, U. S. Ragupathy, P. Vidhyalakshmi, and B. Vinoth, "Inspection of faults in textile web materials using wavelets and ANFIS," in *Machine Vision and Image Processing (MVIP), 2012 International Conference on*, 2012, pp. 189–192.
[14] M. A. K. Jaradat and R. Langari, "A hybrid intelligent system for fault detection and sensor fusion," *Appl. Soft Comput.*, vol. 9, no. 1, pp. 415–422, 2009.
[15] D. Kostadinov and Z. Ivanovski, "Single image depth estimation using local gradient-based features," in *Systems, Signals and Image Processing (IWSSIP), 2012 19th International Conference on*, 2012, pp. 596–599.
[16] S. K. Sinha, P. W. Fieguth, and M. A. Polak, "Computer vision techniques for automatic structural assessment of underground pipes," *Comput. Civ. Infrastruct. Eng.*, vol. 18, no. 2, pp. 95–112, 2003.
[17] M. A. Alam, M. M. N. Ali, M. A. A.-A. Syed, N. Sorif, and M. A. Rahaman, "An algorithm to detect and identify defects of industrial pipes using image processing," in *Software, Knowledge, Information Management and Applications (SKIMA), 2014 8th International Conference on*, 2014, pp. 1–6.
[18] M. R. Islam, M. A. Naser, M. R. Hasan, A. S. M. Shihavuddin, and M. A. Hoque, "Using catadioptric sensor to obtain image of the inner surface of a pipe and detection and analysis of faults by image processing," in *Computer and Information Technology (ICCIT), 2011 14th International Conference on*, 2011, pp. 607–610.
[19] Y. Ganjdanesh, Y. Manjili, M. Vafaei, E. Zamanizadeh, and E. Jahanshahi, "Fuzzy fault detection and diagnosis under severely noisy conditions using feature-based approaches," in *Proceeding of American Control Conference*, 2008, pp. 3319–3324.
[20] M. F. D'Angelo, R. M. Palhares, R. H. Takahashi, R. H. Loschi, L. M. Baccarini, and W. M. Caminhas, "Incipient fault detection in induction machine stator-winding using a fuzzy-Bayesian change point detection approach," *Appl. Soft Comput.*, vol. 11, no. 1, pp. 179–192, 2011.
[21] Y. J. Zhai, X. W. Dai, and Q. Zhou, "Fault detection for gas turbines based on long-term prediction using self-organizing fuzzy neural networks," in *In Machine Learning and Cybernetics*, 2007, pp. 1120–1125.
[22] R. T. Framkot and R. Chellappa, "A method for enforcing integrability in shape from shading algorithms," *IEEE Trans. Pattern Anal. Mach. Intell.*, vol. 4, pp. 439–451, 1988.
[23] "Metal Defects," *Wintress Engineering Corporation*. [Online]. Available: http://www.weco.com/surface-inspection. [Accessed: 29-Jan-2017].
[24] "Metal Can Defects Manual - Identification And Classification," *Canadian Food Inspection Agency*, 2012. [Online]. Available: http://www.inspection.gc.ca/food/fish-and-seafood/manuals/metal-can-defects/eng/1348848316976/134884 9127902.
[25] "Defects- Distributed Porosity," *E- Foundry*. [Online]. Available: http://efoundry.iitb.ac.in/Academy/index.jsp. [Accessed: 29-Jan-2017].
[26] L. J. Olsson and S. Gruber, "Web Process Inspection Using Neural Classification of Scattering Light," *IEEE Trans. Ind. Electron.*, vol. 40, no. 2, pp. 228–234, 1993.
[27] L. W. L. Weiwei, Y. Y. Y. Yunhui, L. J. L. Jun, Z. Y. Z. Yao, and S. H. S. Hongwei, "Automated On-Line Fast Detection for Surface Defect of Steel Strip Based on Multivariate Discriminant Function," *2008 Second Int. Symp. Intell. Inf. Technol. Appl.*, vol. 2, pp. 493–497, 2008.